Since January 2020 Elsevier has created a COVID-19 resource centre with free information in English and Mandarin on the novel coronavirus COVID-19. The COVID-19 resource centre is hosted on Elsevier Connect, the company's public news and information website.

Report

Immunity

PD-1-Expressing SARS-CoV-2-Specific CD8+ T Cells Are Not Exhausted, but Functional in Patients with COVID-19

Graphical Abstract

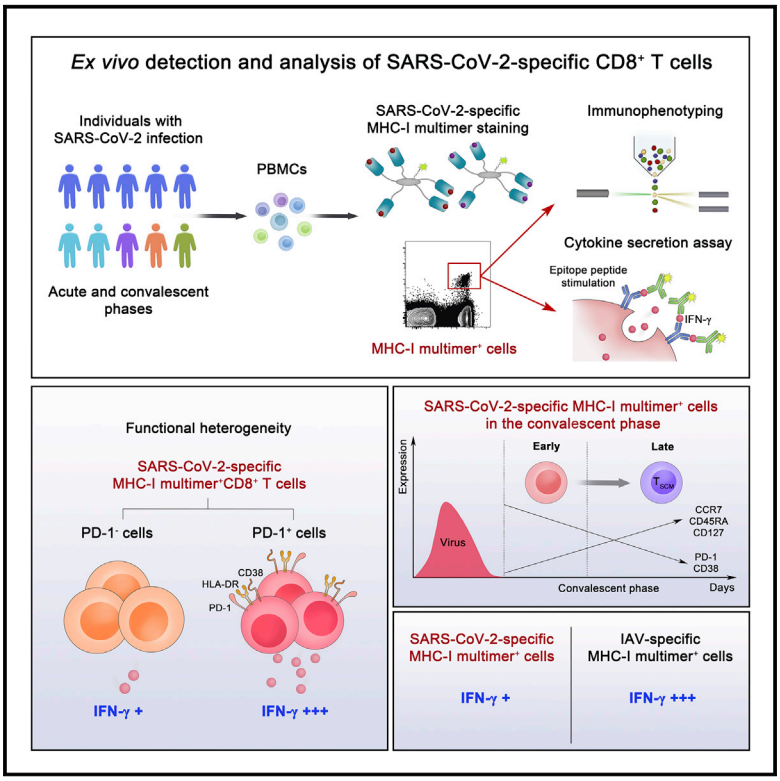

Highlights

- SARS-CoV-2-specific CD8+ T cells are effector memory cells in convalescents
- CCR7+CD45RA+ cells are increased among SARS-CoV-2-specific cells in the late phase
- SARS-CoV-2-specific CD8+ T cells have fewer IFN-γ+ cells than flu-specific cells
- PD-1-expressing SARS-CoV-2-specific CD8+ T cells are not exhausted but functional

Authors

Min-Seok Rha, Hye Won Jeong, Jae-Hoon Ko, ..., Jun Yong Choi, Kyong Ran Peck, Eui-Cheol Shin

Correspondence

cmcws@korea.ac.kr (W.S.C.), seran@yuhs.ac (J.Y.C.), krpeck@skku.edu (K.R.P.), ecshin@kaist.ac.kr (E.-C.S.)

In Brief

T cell responses have been demonstrated in COVID-19 patients, but *ex vivo* phenotypes and functions of SARS-CoV-2-specific T cells remain unclear. Rha et al. examined SARS-CoV-2-specific CD8+ T cells in acute and convalescent COVID-19 patients using MHC class I multimers, finding that PD-1-expressing SARS-CoV-2-specific CD8+ T cells are not exhausted but functional.

Rha et al., 2021, Immunity *54*, 44–52
January 12, 2021
https://doi.org/10.1016/j.immuni.2020.12.002

CellPress

CellPress

Immunity

Report

PD-1-Expressing SARS-CoV-2-Specific CD8$^+$ T Cells Are Not Exhausted, but Functional in Patients with COVID-19

Min-Seok Rha,[1,12] Hye Won Jeong,[2,12] Jae-Hoon Ko,[3,12] Seong Jin Choi,[1] In-Ho Seo,[1] Jeong Seok Lee,[1,4] Moa Sa,[1,5] A Reum Kim,[1] Eun-Jeong Joo,[6] Jin Young Ahn,[7] Jung Ho Kim,[7] Kyoung-Ho Song,[8] Eu Suk Kim,[8] Dong Hyun Oh,[9] Mi Young Ahn,[9] Hee Kyoung Choi,[10] Ji Hoon Jeon,[10] Jae-Phil Choi,[9] Hong Bin Kim,[8] Young Keun Kim,[11] Su-Hyung Park,[1,5] Won Suk Choi,[10,*] Jun Yong Choi,[7,*] Kyong Ran Peck,[3,*] and Eui-Cheol Shin[1,5,13,*]

[1]Graduate School of Medical Science and Engineering, Korea Advanced Institute of Science and Technology (KAIST), Daejeon 34141, Republic of Korea

[2]Department of Internal Medicine, Chungbuk National University College of Medicine, Cheongju 28644, Republic of Korea

[3]Division of Infectious Diseases, Department of Medicine, Samsung Medical Center, Sungkyunkwan University School of Medicine, Seoul 06351, Republic of Korea

[4]GENOME INSIGHT Inc., Daejeon 34051, Republic of Korea

[5]The Center for Epidemic Preparedness, KAIST Institute, Daejeon 34141, Republic of Korea

[6]Division of Infectious Diseases, Department of Internal Medicine, Kangbuk Samsung Hospital, Sungkyunkwan University School of Medicine, Seoul 03181, Republic of Korea

[7]Department of Internal Medicine, Severance Hospital, Yonsei University College of Medicine, Seoul 03722, Republic of Korea

[8]Department of Internal Medicine, Seoul National University Bundang Hospital, Seoul National University College of Medicine, Seongnam 13620, Republic of Korea

[9]Department of Internal Medicine, Seoul Medical Center, Seoul 02053, Republic of Korea

[10]Division of Infectious Diseases, Department of Internal Medicine, Korea University College of Medicine, Ansan Hospital, Ansan 15355, Republic of Korea

[11]Department of Internal Medicine, Wonju Severance Christian Hospital, Yonsei University Wonju College of Medicine, Wonju 26426, Republic of Korea

[12]These authors contributed equally

[13]Lead Contact

*Correspondence: cmcws@korea.ac.kr (W.S.C.), seran@yuhs.ac (J.Y.C.), krpeck@skku.edu (K.R.P.), ecshin@kaist.ac.kr (E.-C.S.)

https://doi.org/10.1016/j.immuni.2020.12.002

SUMMARY

Memory T cell responses have been demonstrated in COVID-19 convalescents, but *ex vivo* phenotypes of SARS-CoV-2-specific T cells have been unclear. We detected SARS-CoV-2-specific CD8$^+$ T cells by MHC class I multimer staining and examined their phenotypes and functions in acute and convalescent COVID-19. Multimer$^+$ cells exhibited early differentiated effector-memory phenotypes in the early convalescent phase. The frequency of stem-like memory cells was increased among multimer$^+$ cells in the late convalescent phase. Cytokine secretion assays combined with MHC class I multimer staining revealed that the proportion of interferon-γ (IFN-γ)-producing cells was significantly lower among SARS-CoV-2-specific CD8$^+$ T cells than those specific to influenza A virus. Importantly, the proportion of IFN-γ-producing cells was higher in PD-1$^+$ cells than PD-1$^-$ cells among multimer$^+$ cells, indicating that PD-1-expressing, SARS-CoV-2-specific CD8$^+$ T cells are not exhausted, but functional. Our current findings provide information for understanding of SARS-CoV-2-specific CD8$^+$ T cells elicited by infection or vaccination.

INTRODUCTION

Coronavirus disease 2019 (COVID-19) is an ongoing pandemic disease caused by infection with severe acute respiratory syndrome coronavirus 2 (SARS-CoV-2). As of August 16, 2020, more than 21 million confirmed cases and more than 760,000 deaths have been reported worldwide (World Health Organization, 2020). COVID-19 is characterized by a broad spectrum of clinical manifestations, ranging from asymptomatic or mild illness to severe illness that requires hospitalization and mechanical ventilation (Huang et al., 2020). To develop effective vaccines and establish appropriate therapeutic interventions for patients with COVID-19, a better understanding of the immune responses against SARS-CoV-2 is urgently needed.

In patients with COVID-19, the CD8$^+$ T cell population undergoes quantitative and qualitative changes. Lymphopenia preferentially affects CD8$^+$ T cells (Mathew et al., 2020; Mazzoni et al., 2020), and low numbers of CD8$^+$ T cells are found in severe

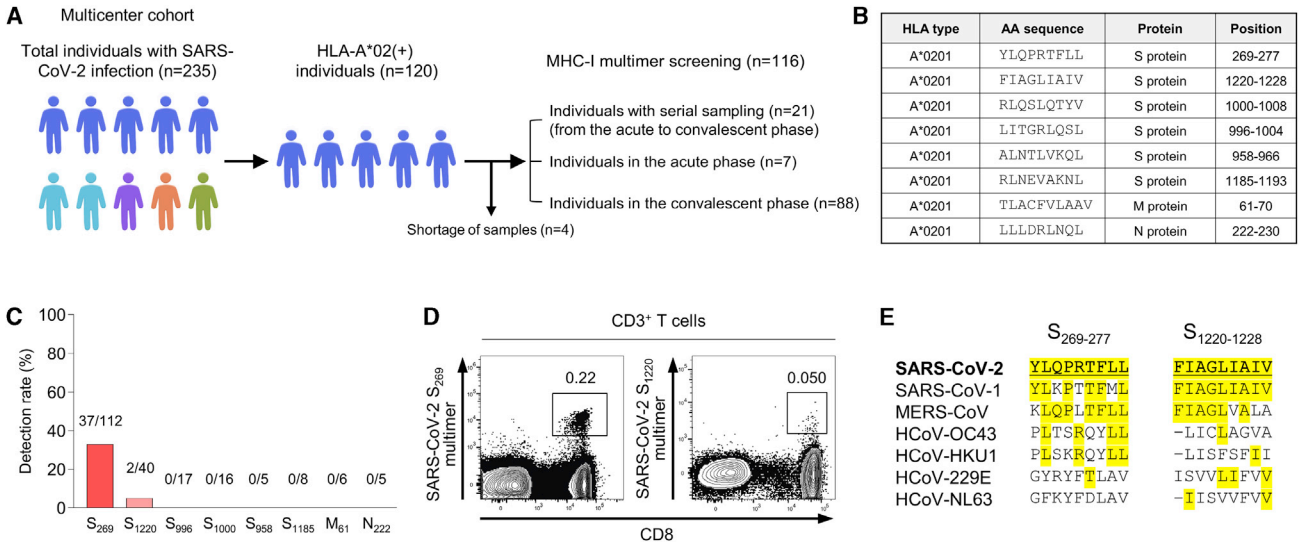

HLA type	AA sequence	Protein	Position
A*0201	YLQPRTFLL	S protein	269-277
A*0201	FIAGLIAIV	S protein	1220-1228
A*0201	RLQSLQTYV	S protein	1000-1008
A*0201	LITGRLQSL	S protein	996-1004
A*0201	ALNTLVKQL	S protein	958-966
A*0201	RLNEVAKNL	S protein	1185-1193
A*0201	TLACFVLAAV	M protein	61-70
A*0201	LLLDRLNQL	N protein	222-230

Figure 1. *Ex Vivo* Detection of SARS-CoV-2-Specific CD8$^+$ T Cells Using MHC Class I Multimers

(A) Study scheme for the detection of SARS-CoV-2-specific MHC class I multimer$^+$CD8$^+$ T cells in PBMCs from individuals with SARS-CoV-2 infection.

(B) SARS-CoV-2-specific MHC class I multimers used in this study.

(C) Summary data for the detection rate of SARS-CoV-2-specific multimer$^+$CD8$^+$ T cells.

(D) Representative flow cytometry plots (S_{269}, n = 37; S_{1220}, n = 2) showing the *ex vivo* detection of SARS-CoV-2 S_{269} and S_{1220} multimer$^+$CD8$^+$ T cells in the gate of CD3$^+$ T cells.

(E) Alignment of the amino acid sequences of SARS-CoV-2 S_{269} and S_{1220} peptides with other human coronaviruses.

See also Figure S1.

diseases (Chen et al., 2020; Mazzoni et al., 2020). In addition, CD8$^+$ T cells from the bronchoalveolar lavage fluid of severe and critical patients exhibit a lack of dominant clones compared with patients with mild COVID-19 (Liao et al., 2020). Several studies have observed an increased frequency of CD38$^+$HLA-DR$^+$ activated CD8$^+$ T cells (Kuri-Cervantes et al., 2020; Mathew et al., 2020) and reduced interferon-γ (IFN-γ) production by CD8$^+$ T cells (Mazzoni et al., 2020; Zheng et al., 2020b) in patients with COVID-19. In addition, a number of studies have reported an exhausted phenotype of CD8$^+$ T cells in severe disease, with increased expression of inhibitory receptors, particularly PD-1 (De Biasi et al., 2020; Diao et al., 2020; Song et al., 2020; Zheng et al., 2020a). However, whether PD-1$^+$CD8$^+$ T cells are truly exhausted or activated in patients with COVID-19 is unclear.

Early studies report SARS-CoV-2-reactive CD8$^+$ T cell responses in individuals with COVID-19 (Grifoni et al., 2020; Le Bert et al., 2020; Weiskopf et al., 2020). Up to 70% of convalescent individuals presented detectable CD8$^+$ T cell responses following *in vitro* stimulation with SARS-CoV-2 overlapping peptides (Grifoni et al., 2020). These studies utilized activation-induced marker (e.g., 4-1BB) assays or stimulation-based functional assays, such as IFN-γ ELISpot assays and intracellular cytokine staining, to detect SARS-CoV-2-reactive CD8$^+$ T cell responses (Grifoni et al., 2020; Le Bert et al., 2020; Weiskopf et al., 2020).

However, these assays have inherent limitations for the proper characterization of SARS-CoV-2-specific CD8$^+$ T cells. Stimulation-based functional assays cannot detect virus-specific CD8$^+$ T cells that are not functioning, and phenotypes of CD8$^+$ T cells can change during *in vitro* stimulation. The limitation of stimulation-based functional assays can be overcome by using major histocompatibility complex class I (MHC class I) multimer techniques (Altman et al., 1996). A recent study has detected SARS-CoV-2-specific CD8$^+$ T cells using MHC class I multimers and described their phenotypes (Sekine et al., 2020). However, functional heterogeneity within the SARS-CoV-2-specific CD8$^+$ T cell population has not been elucidated in acute and convalescent COVID-19 patients. For example, little information is known as to whether PD-1$^+$ cells among SARS-CoV-2-specific MHC class I multimer$^+$CD8$^+$ T cells are functioning or exhausted.

In the present study, we detected SARS-CoV-2-specific CD8$^+$ T cells using MHC class I multimers and investigated their *ex vivo* phenotypes in peripheral blood mononuclear cells (PBMCs) from acute and convalescent COVID-19 patients. We also performed cytokine secretion assays (CSAs) combined with MHC class I multimer staining for *ex vivo* functional analysis of SARS-CoV-2-specific CD8$^+$ T cells. Our current analysis provides information that is required for understanding of SARS-CoV-2-specific CD8$^+$ T cells elicited by infection or vaccination.

RESULTS

MHC Class I Multimer Staining Identifies a Dominant CD8$^+$ T Cell Epitope in SARS-CoV-2

We recruited a multicenter cohort comprised of 235 patients with SARS-CoV-2 infection, including 120 who were HLA-A*02(+). After excluding 4 patients due to a shortage of PBMC specimens, we analyzed PBMCs from 116 HLA-A*02(+) patients. Serial blood samples from the acute to convalescent phase were collected from 21 of these patients, and a single blood sample was taken in the acute phase from 7 patients and in the convalescent phase from 88 patients (Figure 1A). We used eight commercially

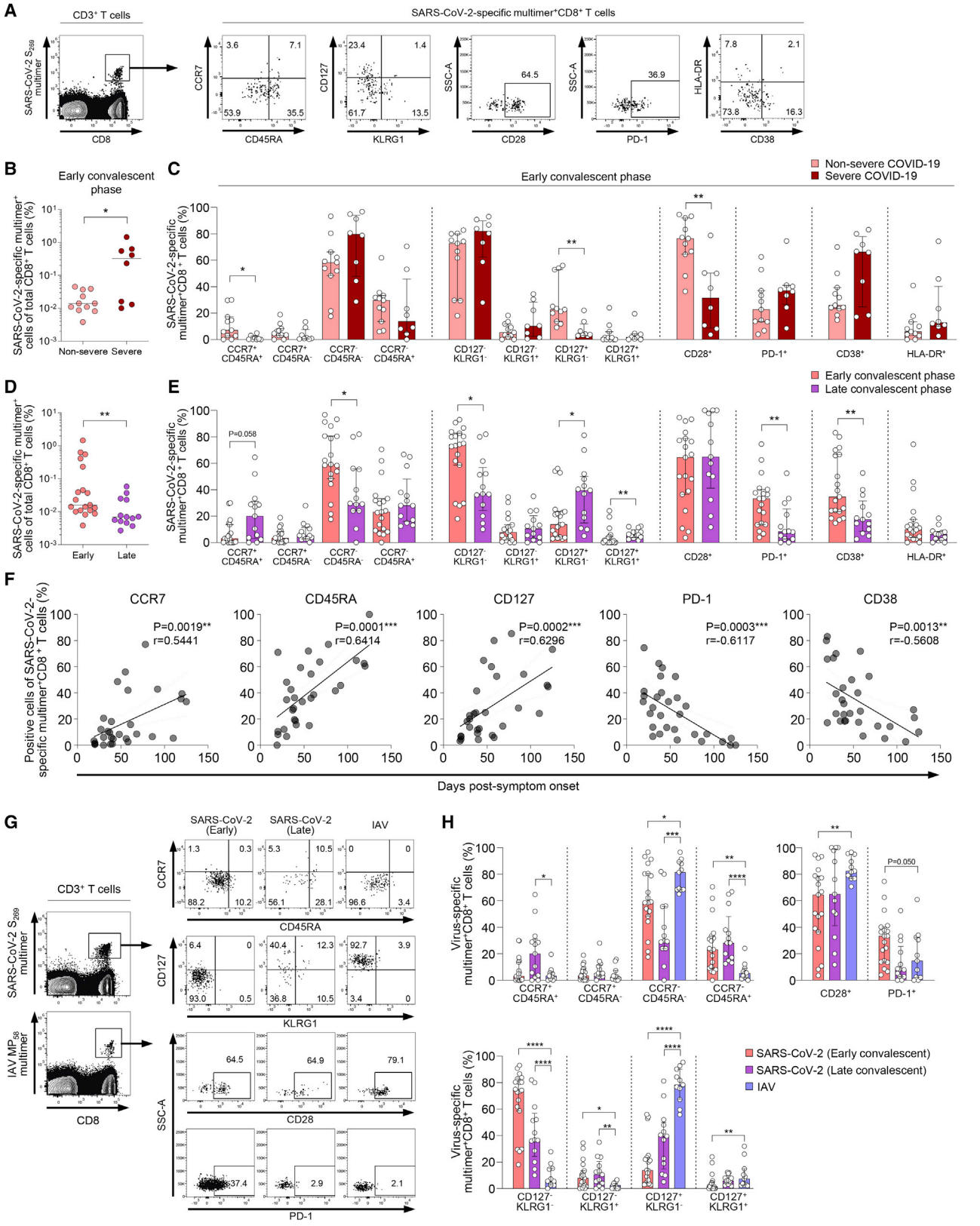

(legend on next page)

available HLA-A*02 multimers for the detection of SARS-CoV-2-specific CD8$^+$ T cells: six for spike (S) protein, one for membrane (M) protein, and one for nucleocapsid (N) protein (Figure 1B). SARS-CoV-2 S_{269} (YLQPRTFLL) multimer$^+$ cells were detected in 37 of 112 (33.04%) patients, and SARS-CoV-2 S_{1220} (FIAGLIAIV) multimer$^+$ cells in 2 of 40 (5.0%) patients (Figures 1C and 1D). The demographic and clinical characteristics of the patients with multimer$^+$ cells are presented in Table S1. However, multimer$^+$ cells were undetectable when staining the other MHC class I multimers (Figure 1C). We found that SARS-CoV-2 S_{269} and S_{1220} had a low degree of homology to the sequences of human common cold coronaviruses, including OC43, HKU1, 229E, and NL63 (Figure 1E). The S_{269} epitope was specific to SARS-CoV-2, whereas the S_{1220} epitope was conserved in SARS-CoV-1 (Figure 1E). SARS-CoV-2 S_{269} or S_{1220} MHC class I multimer$^+$ cells were not detected in PBMCs from HLA-A*02(+) subjects without SARS-CoV-2 infection (Figure S1).

SARS-CoV-2-Specific CD8$^+$ T Cells Are Mainly Effector Memory Cells in the Convalescent Phase

We examined the *ex vivo* phenotypes of SARS-CoV-2 S_{269} MHC class I multimer$^+$CD8$^+$ T cells in PBMCs from convalescent individuals by assessing the expression of the chemokine receptor CCR7 and CD45RA. MHC class I multimer$^+$ cells predominantly exhibited an effector memory (CCR7$^-$CD45RA$^-$) phenotype, and roughly 25% of MHC class I multimer$^+$ cells were terminally differentiated effector (CCR7$^-$CD45RA$^+$) cells (Figures 2A and S2). Some patients had a considerable proportion of CCR7$^+$CD45RA$^+$ cells among the MHC class I multimer$^+$ cells, which may indicate the presence of CD8$^+$ stem-like memory T cells (Gattinoni et al., 2011).

During viral infection, CD127 and KLRG1 have been used as markers to identify effector CD8$^+$ T cell subsets with distinct features regarding long-term survival and effector function (Chang et al., 2014). We found that the majority of MHC class I multimer$^+$ cells from convalescent individuals were CD127$^-$KLRG1$^-$ cells (Figures 2A and S2). In addition, a considerable proportion of MHC class I multimer$^+$ cells were CD127$^-$KLRG1$^+$ and CD127$^+$KLRG1$^-$ cells, whereas CD127$^+$KLRG1$^+$ cells were rarely observed (Figures 2A and S2).

The expression of CD28 is particularly useful in distinguishing between subsets of differentiated CD8$^+$ T cells (Appay et al., 2002). The MHC class I multimer$^+$ cells in our cohort were largely CD28$^+$ cells, suggesting that these cells are early differentiated cells (Figures 2A and S2). When we examined T cell exhaustion and activation markers, the frequencies of PD-1$^+$, CD38$^+$, and HLA-DR$^+$ cells among MHC class I multimer$^+$ cells were approximately 20%, 25%, and 10%, respectively (Figures 2A and S2).

We classified the convalescent PBMC samples into two groups, "early convalescent" and "late convalescent", obtained within and after the first 14 days following the negative conversion of viral RNA in nasopharyngeal swab specimens, respectively. First, we analyzed the early convalescent samples and compared the frequency and phenotype of MHC class I multimer$^+$ cells between the two groups according to disease severity (n = 11 non-severe and n = 8 severe). The severe group had a significantly higher frequency of MHC class I multimer$^+$ cells among CD8$^+$ T cells than the non-severe group (Figure 2B). The frequency of CD127$^+$KLRG1$^-$ and CD28$^+$ cells among MHC class I multimer$^+$ cells was significantly lower in the severe group than the non-severe group (Figure 2C).

Stem-like Memory Cells Are Increased among SARS-CoV-2-Specific CD8$^+$ T Cells in the Late Convalescent Phase

Next, we compared the frequency and phenotype of MHC class I multimer$^+$ cells between the early convalescent and late convalescent samples. The frequency of MHC class I multimer$^+$ cells among CD8$^+$ T cells was higher in the early convalescent samples than the late convalescent samples (Figure 2D). The percentage of CCR7$^+$CD45RA$^+$ cells tended to be higher in the late convalescent samples, whereas the percentage of CCR7$^-$CD45RA$^-$ cells was significantly decreased (Figure 2E). In addition, the frequency of CD127$^+$KLRG1$^-$ cells among MHC class I multimer$^+$ cells was significantly increased in the late convalescent samples, whereas the frequency of CD127$^-$KLRG1$^-$ cells was decreased (Figure 2E). We also observed that the expression of PD-1 and CD38 in MHC class I multimer$^+$ cells was lower in the late convalescent samples compared to the early convalescent samples (Figure 2E). When we investigated the correlation between phenotypes of MHC class I multimer$^+$ cells and days post-symptom onset, the percentage of CCR7$^+$, CD45RA$^+$, and CD127$^+$ cells among MHC class I multimer$^+$ cells positively correlated with the timing (Figure 2F), indicating that stem-like memory CD8$^+$ T cells may be generated in the late convalescent phase. Furthermore, we observed an inverse correlation between the expression of PD-1 and CD38 in MHC class I multimer$^+$ cells and days post-symptom onset (Figure 2F).

We further compared SARS-CoV-2-specific CD8$^+$ T cells with influenza A virus (IAV)-specific CD8$^+$ T cells in terms of the differentiation phenotype. The IAV-specific CD8$^+$ T cell population

Figure 2. Phenotypes of SARS-CoV-2-Specific Multimer$^+$CD8$^+$ T Cells in the Convalescent Phase of COVID-19

(A–H) PBMCs from convalescent patients were analyzed by flow cytometry.

(A) Representative flow cytometry plots (n = 32) showing the percentages of indicated subsets among SARS-CoV-2 S_{269} multimer$^+$CD8$^+$ T cells.

(B and C) The frequency of SARS-CoV-2 S_{269} multimer$^+$CD8$^+$ T cells among total CD8$^+$ T cells (B) and the percentages of the indicated subsets among SARS-CoV-2 S_{269} multimer$^+$CD8$^+$ T cells (C) in the early convalescent samples were compared between the non-severe (n = 11) and severe (n = 8) groups.

(D and E) The frequency of SARS-CoV-2 S_{269} multimer$^+$CD8$^+$ T cells among total CD8$^+$ T cells (D) and the percentages of the indicated subsets among SARS-CoV-2 S_{269} multimer$^+$CD8$^+$ T cells (E) were compared between the early (n = 19) and late (n = 13) convalescent groups.

(F) Correlation between the expression of the indicated markers in SARS-CoV-2 S_{269} multimer$^+$CD8$^+$ T cells and days post-symptom onset (n = 30).

(G and H) The phenotypes of SARS-CoV-2 S_{269} multimer$^+$CD8$^+$ T cells (early convalescent phase, n = 19; late convalescent phase, n = 13) were compared with those of IAV MP_{58} multimer$^+$CD8$^+$ T cells (n = 11; 3 HDs and 8 convalescent individuals). Representative flow cytometry plots (early convalescent phase, n = 19; late convalescent phase, n = 13; IAV, n = 11) (G) and summary data (H) of the percentages of all indicated subsets among CD8$^+$ T cells specific for each virus. Data are presented as median and interquartile range (IQR). Statistical analysis was performed using the Mann–Whitney U test (B–E and H) or Spearman correlation test (F). *p < 0.05, **p < 0.01, ***p < 0.001, ****p < 0.0001. See also Figure S2.

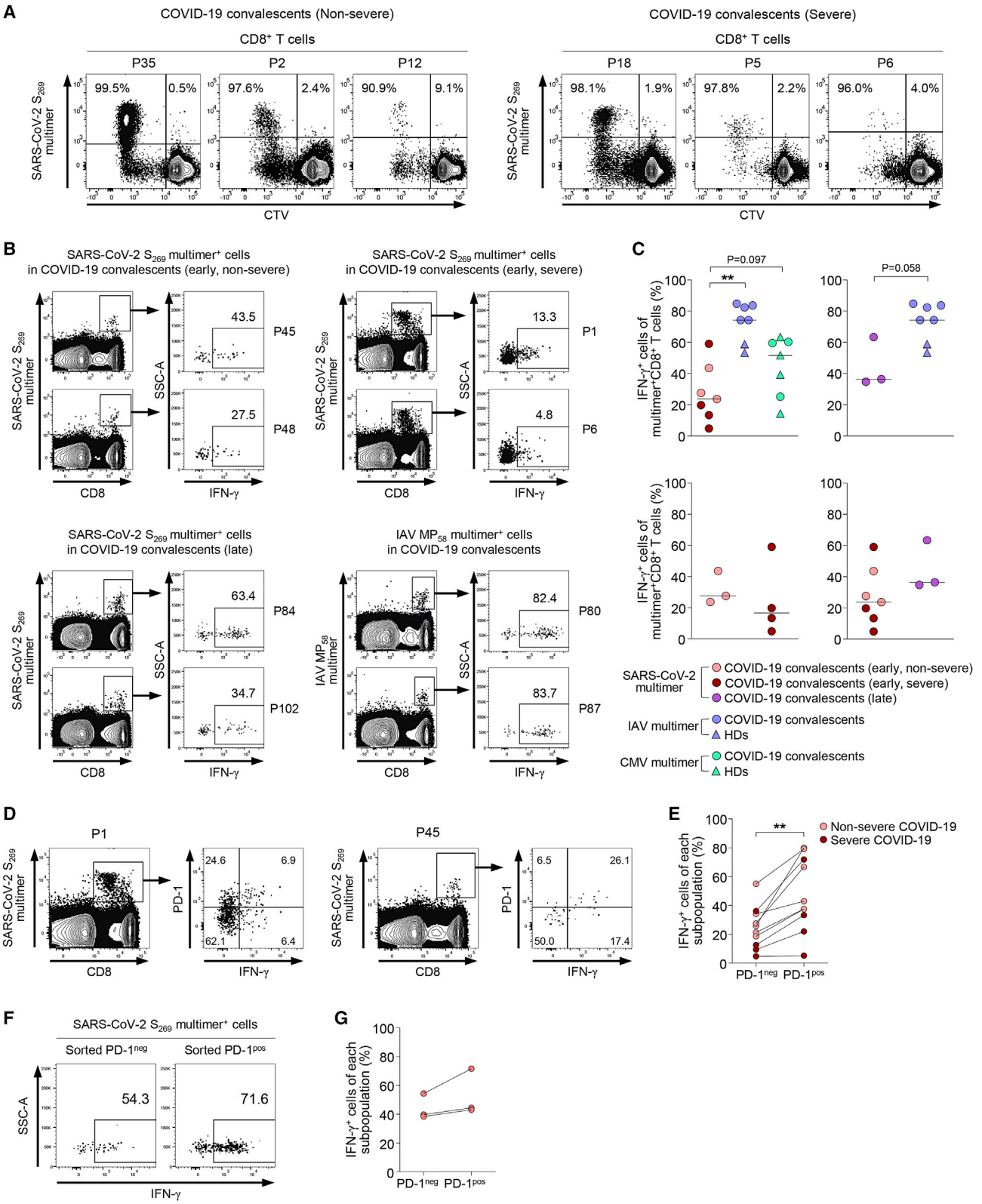

Figure 3. Proliferation and Effector Function of SARS-CoV-2-Specific CD8+ T Cells from Convalescent Patients

(A) CTV-labeled PBMCs from convalescent COVID-19 patients (n = 6) were stimulated with S_{269} peptide (10 μg/mL) for 7 days and analyzed by flow cytometry. Flow cytometry plots show the frequency of CTV^{low} cells among SARS-CoV-2 S_{269} multimer+$CD8^+$ T cells.

(legend continued on next page)

(n = 11; 3 healthy donors [HDs] and 8 convalescent patients) had more $CD127^+KLRG1^-$ and $CCR7^-CD45RA^-$ cells than the SARS-CoV-2-specific $CD8^+$ T cell population from both early (n = 19) and late (n = 13) convalescent samples (Figures 2G and 2H). In contrast, the frequency of $CCR7^+CD45RA^+$ cells was higher in SARS-CoV-2-specific $CD8^+$ T cells from the late convalescent samples compared with IAV-specific $CD8^+$ T cells (Figures 2G and 2H). The expression of PD-1 tended to be lower in IAV-specific $CD8^+$ T cells compared with SARS-CoV-2-specific $CD8^+$ T cells from early convalescent samples, but the difference was not significant (Figures 2G and 2H).

PD-1-Expressing SARS-CoV-2-Specific $CD8^+$ T Cells Are Not Exhausted but Functional

To evaluate the memory response of $CD8^+$ T cells following resolution of the infection, we analyzed the proliferative capacity of SARS-CoV-2-specific $CD8^+$ T cells from convalescent patients. PBMCs from convalescent patients were stimulated with S_{269} peptide, and the proliferation of SARS-CoV-2 S_{269} multimer$^+CD8^+$ T cells was evaluated by CellTrace Violet (CTV) dilution assays. We confirmed that SARS-CoV-2 S_{269}-specific memory $CD8^+$ T cells have the capacity to proliferate upon antigenic re-challenge regardless of the disease severity (Figure 3A).

Next, we investigated IFN-γ production from SARS-CoV-2-specific MHC class I multimer$^+CD8^+$ T cells. We stimulated PBMCs from convalescent patients with S_{269} peptide *ex vivo* and performed CSAs with SARS-CoV-2 S_{269} multimer staining for simultaneous analysis of the phenotype and function of virus-specific T cells (Park et al., 2012). Comparing IFN-γ production by SARS-CoV-2-specific $CD8^+$ T cells from individuals in the early convalescent phase and $CD8^+$ T cells specific for IAV or cytomegalovirus (CMV) from convalescent individuals or HDs, we found that the proportion of IFN-γ-producing cells was significantly lower in SARS-CoV-2 multimer$^+$ cells than in IAV multimer$^+$ cells (n = 7 versus n = 7 and n = 7, IAV [2 HDs and 5 convalescent patients] and CMV [4 HDs and 3 convalescent patients], respectively; Figures 3B and 3C). We also observed that the proportion of IFN-γ^+ cells tended to be lower in SARS-CoV-2 multimer$^+$ cells from the late convalescent samples compared with IAV multimer$^+$ cells (Figures 3B and 3C). In addition, we found no significant differences in the frequency of IFN-γ-producing cells among SARS-CoV-2 multimer$^+$ cells between early convalescent samples from the severe group and those from the non-severe group or between the early convalescent and late convalescent samples (Figures 3B and 3C).

Because a considerable proportion of the SARS-CoV-2-specific multimer$^+CD8^+$ T cell population expressed PD-1 (Figures 2A and S2), we investigated whether IFN-γ was produced by PD-1^+ or PD-1^- cells among SARS-CoV-2-specific multimer$^+$ $CD8^+$ T cells. The proportion of IFN-γ-producing cells was significantly higher in PD-1^+ cells than in PD-1^- cells regardless of disease severity (Figures 3D and 3E). To confirm this result, we performed IFN-γ CSAs after sorting PD-1^+CD8^+ and PD-1^-CD8^+ T cells. MHC class I multimer$^+$ cells among sorted PD-1^+CD8^+ T cells, as well as those among sorted PD-1^-CD8^+ T cells, produced IFN-γ (Figures 3F and 3G). These findings demonstrate that PD-1-expressing SARS-CoV-2-specific MHC class I multimer$^+$ cells are not exhausted but functional in patients with COVID-19.

Frequency and Phenotypes of SARS-CoV-2-Specific $CD8^+$ T Cells Change during Viral Clearance in the Acute Phase

Next, we examined the phenotype of SARS-CoV-2-specific multimer$^+CD8^+$ T cells in the acute phase of COVID-19. Multimer$^+$ cells from patients in the acute phase exhibited an activated phenotype with high expression of CD38, HLA-DR, and PD-1 (Figure 4A). Almost all of the multimer$^+$ cells expressed cytotoxic molecules, including perforin and granzyme B (Figure 4A). In addition, the proliferation marker Ki-67 was highly expressed in multimer$^+$ cells in the acute phase, whereas CD127, a marker of memory precursor cells, was rarely expressed (Figure 4A).

We also studied the kinetics of the *ex vivo* phenotypes of SARS-CoV-2-specific multimer$^+CD8^+$ T cells during the course of COVID-19. Viral titer measured by real-time reverse-transcription (RT)-PCR detection of the SARS-CoV-2 viral genome in nasopharyngeal swab samples tended to decrease over time (Figure 4B). In addition, the frequency of multimer$^+$ cells among total $CD8^+$ T cells tended to follow the viral titer kinetics (Figure 4B). The proportions of Ki-67^+ proliferating cells and $CD38^+HLA\text{-}DR^+$ activated cells among multimer$^+$ cells paralleled changes in the frequency of multimer$^+$ cells (Figure 4B). However, the proportions of perforin$^+$granzyme B^+ cells and PD-1^+ cells among multimer$^+$ cells tended to be sustained during the course of COVID-19 (Figure 4B).

Finally, we performed CSAs with MHC class I multimer staining to examine which subpopulations of multimer$^+$ cells produce IFN-γ in the acute phase. Within the SARS-CoV-2-specific multimer$^+CD8^+$ T cell population, IFN-γ^+ cells were more frequently observed among PD-1^+ cells compared with PD-1^- cells (Figures 4C and 4D). In the analysis with activation markers, IFN-γ was also produced mainly by $CD38^+$ or $HLA\text{-}DR^+$ cells (Figures 4C and 4D). These data indicate that IFN-γ is produced by

(B–E) PBMCs were stimulated with SARS-CoV-2 S_{269} peptide (n = 10; 3 early convalescent samples with non-severe disease, 4 early convalescent samples with severe disease, and 3 late convalescent samples), CMV $pp65_{495}$ peptide (n = 7; 4 HDs and 3 convalescent individuals), or IAV MP_{58} peptide (n = 7; 2 HDs and 5 convalescent individuals). The concentration of each peptide was 1 μg/mL. After 5.5 h of stimulation, CSAs were performed in combination with MHC class I multimer staining to analyze the frequency of IFN-γ-producing cells among MHC class I multimer$^+$ cells. Representative flow cytometry plots (early convalescent samples with non-severe disease, n = 3; early convalescent samples with severe disease, n = 4; late convalescent samples, n = 3; IAV, n = 7) (B) and summary data (C) are presented. Horizontal lines represent the median. (D) Representative flow cytometry plots (n = 10) and (E) summary data showing the frequency of IFN-γ-producing cells among PD-1^+ and PD-1^- subpopulations of SARS-CoV-2 S_{269} multimer$^+CD8^+$ T cells from convalescent COVID-19 patients.
(F and G) Sorted PD-1^+CD8^+ and sorted PD-1^-CD8^+ T cells from PBMCs of COVID-19 patients (n = 3) were stimulated with SARS-CoV-2 S_{269} peptide (1 μg/mL) for 5.5 h and CSAs performed in combination with MHC class I multimer staining. Representative flow cytometry plots (n = 3) (F) and summary data (G) showing the frequency of IFN-γ-producing cells in the SARS-CoV-2 S_{269} multimer$^+CD8^+$ T cell population among sorted PD-1^+ and PD-1^-CD8^+ T cells.
Statistical analysis was performed using the Mann–Whitney U test (C) or the Wilcoxon signed-rank test (E). $^{**}p < 0.01$.

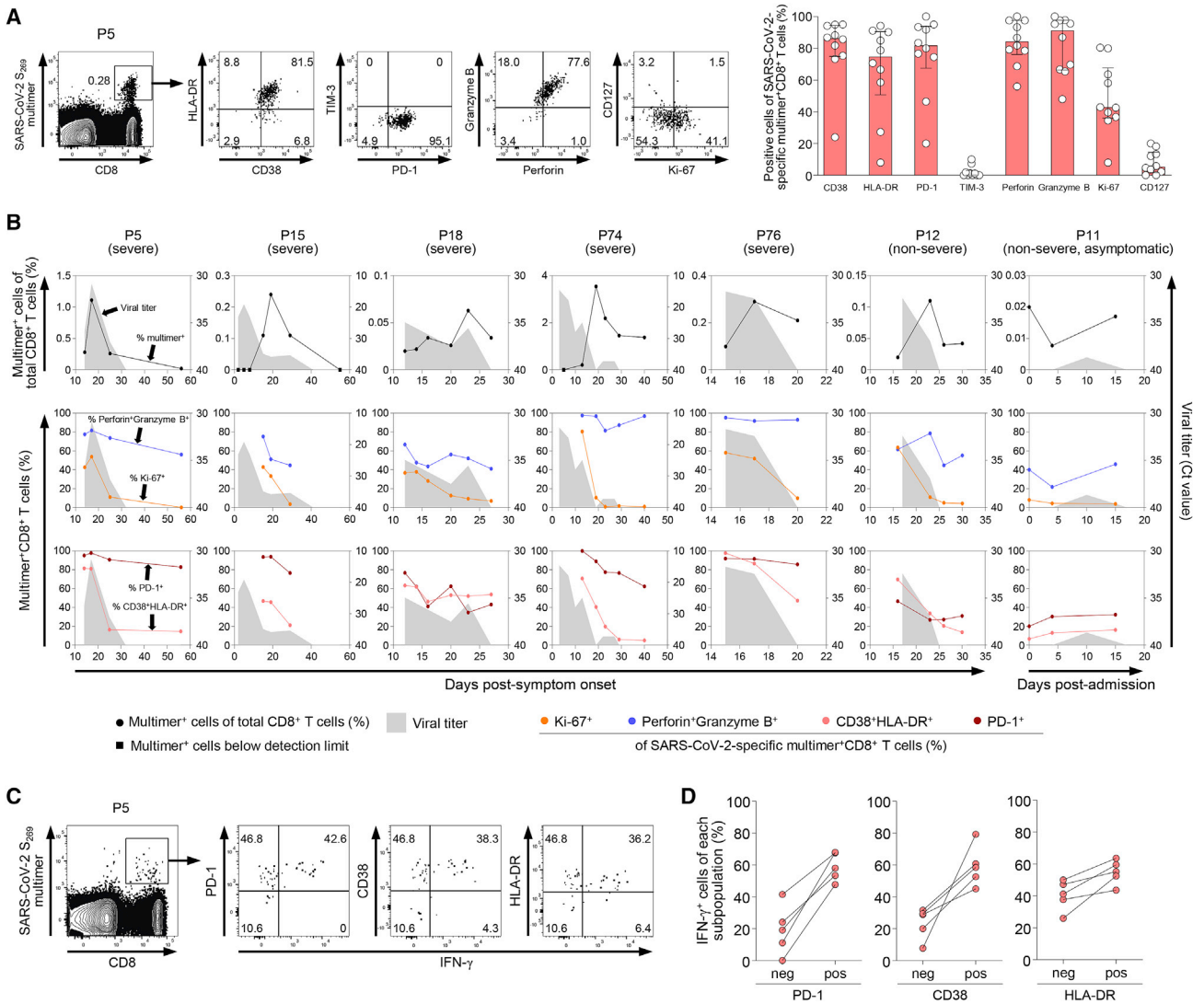

Figure 4. Phenotypes, Kinetics, and Effector Function of SARS-CoV-2-Specific Multimer$^+$CD8$^+$ T Cells in the Acute Phase of COVID-19.

(A) PBMCs from patients in the acute phase of COVID-19 (n = 10) were analyzed by flow cytometry. Left, Representative flow cytometry plots (n = 10). Right, summary data for the expression of indicated markers in SARS-CoV-2 S_{269} multimer$^+$CD8$^+$ T cells. Data are presented as median and IQR.

(B) The frequency and phenotypes of SARS-CoV-2-specific CD8$^+$ T cells were examined during the course of SARS-CoV-2 infection in seven patients (P5, P15, P18, P74, and P76, severe disease; P12, non-severe disease; and P11, non-severe, asymptomatic). Viral titers (Ct values) were determined by real-time RT-PCR of RdRP (P5, P15, P18, P74, P76, and P12) or N (P11) genes in specimens from nasopharyngeal swabs serially obtained during the course of COVID-19. The viral titer and frequency of SARS-CoV-2 S_{269} multimer$^+$ cells among total CD8$^+$ T cells were plotted against days post-symptom onset (P5, P15, P18, P74, P76, and P12) or days post-admission (P11). The percentages of Ki-67$^+$ (orange), perforin$^+$granzyme B$^+$ (blue), CD38$^+$HLA-DR$^+$ (pink), and PD-1$^+$ (dark red) cells among multimer$^+$ cells are presented.

(C and D) PBMCs from P5 (14 days post-symptom onset), P12 (16 days post-symptom onset), P15 (15 days post-symptom onset), P74 (19 days post-symptom onset), and P76 (17 days post-symptom onset) were stimulated with S_{269} peptide (1 μg/mL) for 5.5 h and CSAs performed in combination with MHC class I multimer staining to analyze the phenotypes of IFN-γ-producing cells among MHC class I multimer$^+$ cells. Representative flow cytometry plots (n = 5) (C) and summary data (D) show IFN-γ production according to the expression of PD-1, CD38, and HLA-DR in the gate of multimer$^+$ cells.

activated SARS-CoV-2-specific CD8$^+$ T cells, and that PD-1-expressing SARS-CoV-2-specific CD8$^+$ T cells are activated functioning cells, not exhausted cells, in the acute phase of COVID-19.

DISCUSSION

In the present study, we utilized an MHC class I multimer technique to detect SARS-CoV-2-specific CD8$^+$ T cells and investigated the *ex vivo* phenotypes and function of SARS-CoV-2-specific CD8$^+$ T cells in combination with CSAs in the acute and convalescent phases of COVID-19. Notably, SARS-CoV-2-specific memory CD8$^+$ T cells from convalescent patients exhibited a high proliferative capacity, but IFN-γ was produced by less than half of the SARS-CoV-2-specific memory CD8$^+$ T cell population. We also demonstrated that PD-1-expressing SARS-CoV-2-specific CD8$^+$ T cells from acute and

convalescent patients were not exhausted, but activated and functional.

A key feature of T cell exhaustion is loss of effector function with sustained expression of inhibitory receptors (McLane et al., 2019; Wherry and Kurachi, 2015). However, inhibitory receptors are also upregulated in effector $CD8^+$ T cells by T cell receptor-induced activation (Singer et al., 2016; Wherry and Kurachi, 2015). Although many studies have suggested exhausted phenotypes of $CD8^+$ T cells on the basis of increased PD-1 expression in patients with COVID-19 (De Biasi et al., 2020; Song et al., 2020; Zheng et al., 2020a; Zheng et al., 2020b), whether $CD8^+$ T cells truly become exhausted remains controversial. In the current study, we demonstrated that PD-1^+ cells are not dysfunctional in the acute or convalescent phase of COVID-19. From these results, we conclude that the PD-1 expression on $CD8^+$ T cells likely reflects activation, rather than exhaustion, in COVID-19.

Another gap in our current understanding is how T cell memory forms in patients who experience mild versus severe COVID-19. In the current study, we found that the frequency of $CD127^+KLRG1^-$ cells, which are known as memory-precursor effector cells during viral infection and able to differentiate into multiple memory cell lineages (Chang et al., 2014; Kaech and Wherry, 2007), among SARS-CoV-2-specific $CD8^+$ T cells was significantly lower in individuals who recently recovered from severe disease than those who recovered from mild disease. These data indicate that there may be differences in $CD8^+$ T cell memory formation between patients who experienced mild versus severe COVID-19. Whether the generation of long-term memory $CD8^+$ T cells is influenced by disease severity during the acute phase of COVID-19 remains to be investigated.

Currently, many efforts are underway to develop prophylactic vaccines against SARS-CoV-2 by inducing neutralizing antibodies and memory T cells. However, the phenotypes of vaccine-induced, SARS-CoV-2-specific memory $CD8^+$ T cells have not been investigated. Previously, MHC class I multimers were used to extensively examine the phenotypes and functions of vaccine-induced, virus-specific memory $CD8^+$ T cells in a chimpanzee model of hepatitis C virus infection (Park et al., 2012; Shin et al., 2013). In this model, vaccine-induced memory $CD8^+$ T cells exhibited higher CD127 expression and polyfunctionality than infection-induced memory $CD8^+$ T cells (Park et al., 2012). In the current study, we found that the SARS-CoV-2-specific memory $CD8^+$ T cell population from convalescent patients exhibited low CD127 expression and had a low frequency of IFN-γ-producing cells. These findings indicate that memory $CD8^+$ T cells generated during natural infection may have suboptimal responses against re-infection; thus, vaccination may be required to develop effective T cell memory.

In summary, we characterized the immunological features of SARS-CoV-2-specific $CD8^+$ T cells in acute and convalescent COVID-19 patients. Our data provide insights into SARS-CoV-2-specific $CD8^+$ T cell responses and $CD8^+$ T cell memory in the acute and convalescent phases of COVID-19. Given that $CD8^+$ T cells act as cardinal sentinels against viral infections, these results may fill gaps in current knowledge for the development of prophylactics and therapeutics against SARS-CoV-2 infection and for controlling the current COVID-19 pandemic.

Limitations of Study

Caveats of this study include the relatively low sample size. While we screened a total of 235 individuals with COVID-19, larger cohorts are needed to obtain clear results. Herein, we suggest the evolution of SARS-CoV-2-specific $CD8^+$ T cells into stem-like memory cells in the late convalescent phase. However, it needs to be confirmed by definitive markers of stem-like memory cells, including CD95. In addition, future studies with long-term follow-up of COVID-19 convalescents would be required for a better comparison between SARS-CoV-2-specific memory T cells and memory T cells specific to other viruses. Our study relies on MHC class I multimers specific to HLA-A*02-restricted epitopes in S protein. However, $CD8^+$ T cells specific to other SARS-CoV-2 proteins and epitopes restricted by other HLA class I allotypes might differ in phenotypes and function, which should be addressed in further studies.

STAR★METHODS

Detailed methods are provided in the online version of this paper and include the following:

- KEY RESOURCES TABLE
- RESOURCE AVAILABILITY
  - Lead Contact
  - Materials Availability
  - Data and Code Availability
- EXPERIMENTAL MODEL AND SUBJECT DETAILS
  - Patients and Specimens
- METHOD DETAILS
  - MHC class I multimer staining and multi-color flow cytometry
  - Sequence alignment
  - Cell sorting
  - Cytokine secretion assay
  - Proliferation assay
  - Statistical analysis

SUPPLEMENTAL INFORMATION

Supplemental Information can be found online at https://doi.org/10.1016/j.immuni.2020.12.002.

ACKNOWLEDGMENTS

This work was supported by the Samsung Science and Technology Foundation under Project Number SSTF-BA1402-51.

AUTHOR CONTRIBUTIONS

M.-S.R., H.W.J., J.-H.K., W.S.C., J.Y.C., K.R.P., and E.-C.S. designed the research. H.W.J., J.-H.K., E.-J.J., J.Y.A., J.H.K., K.-H.S., E.S.K., D.H.O., M.Y.A., H.K.C., J.H.J., J.-P.C., H.B.K., Y.K.K., W.S.C., J.Y.C., and K.R.P. collected clinical specimens. M.-S.R., S.J.C., I.-H.S., J.S.L., M.S., and A.R.K. performed experiments. M.-S.R., S.-H.P., and E.-C.S. analyzed the results. M.-S.R. and E.-C.S. wrote the manuscript.

DECLARATION OF INTERESTS

The authors have no conflicts of interest.

Received: August 24, 2020
Revised: November 1, 2020
Accepted: December 3, 2020
Published: December 10, 2020

REFERENCES

Altman, J.D., Moss, P.A., Goulder, P.J., Barouch, D.H., McHeyzer-Williams, M.G., Bell, J.I., McMichael, A.J., and Davis, M.M. (1996). Phenotypic analysis of antigen-specific T lymphocytes. Science *274*, 94–96.

Appay, V., Dunbar, P.R., Callan, M., Klenerman, P., Gillespie, G.M., Papagno, L., Ogg, G.S., King, A., Lechner, F., Spina, C.A., et al. (2002). Memory CD8+ T cells vary in differentiation phenotype in different persistent virus infections. Nat. Med. *8*, 379–385.

Chang, J.T., Wherry, E.J., and Goldrath, A.W. (2014). Molecular regulation of effector and memory T cell differentiation. Nat. Immunol. *15*, 1104–1115.

Chen, G., Wu, D., Guo, W., Cao, Y., Huang, D., Wang, H., Wang, T., Zhang, X., Chen, H., Yu, H., et al. (2020). Clinical and immunological features of severe and moderate coronavirus disease 2019. J. Clin. Invest. *130*, 2620–2629.

De Biasi, S., Meschiari, M., Gibellini, L., Bellinazzi, C., Borella, R., Fidanza, L., Gozzi, L., Iannone, A., Lo Tartaro, D., Mattioli, M., et al. (2020). Marked T cell activation, senescence, exhaustion and skewing towards TH17 in patients with COVID-19 pneumonia. Nat. Commun. *11*, 3434.

Diao, B., Wang, C., Tan, Y., Chen, X., Liu, Y., Ning, L., Chen, L., Li, M., Liu, Y., Wang, G., et al. (2020). Reduction and Functional Exhaustion of T Cells in Patients With Coronavirus Disease 2019 (COVID-19). Front. Immunol. *11*, 827.

Edgar, R.C. (2004). MUSCLE: multiple sequence alignment with high accuracy and high throughput. Nucleic Acids Res. *32*, 1792–1797.

Gattinoni, L., Lugli, E., Ji, Y., Pos, Z., Paulos, C.M., Quigley, M.F., Almeida, J.R., Gostick, E., Yu, Z., Carpenito, C., et al. (2011). A human memory T cell subset with stem cell-like properties. Nat. Med. *17*, 1290–1297.

Grifoni, A., Weiskopf, D., Ramirez, S.I., Mateus, J., Dan, J.M., Moderbacher, C.R., Rawlings, S.A., Sutherland, A., Premkumar, L., Jadi, R.S., et al. (2020). Targets of T Cell Responses to SARS-CoV-2 Coronavirus in Humans with COVID-19 Disease and Unexposed Individuals. Cell *181*, 1489–1501.e15.

Huang, C., Wang, Y., Li, X., Ren, L., Zhao, J., Hu, Y., Zhang, L., Fan, G., Xu, J., Gu, X., et al. (2020). Clinical features of patients infected with 2019 novel coronavirus in Wuhan, China. Lancet *395*, 497–506.

Kaech, S.M., and Wherry, E.J. (2007). Heterogeneity and cell-fate decisions in effector and memory CD8+ T cell differentiation during viral infection. Immunity *27*, 393–405.

Kuri-Cervantes, L., Pampena, M.B., Meng, W., Rosenfeld, A.M., Ittner, C.A.G., Weisman, A.R., Agyekum, R.S., Mathew, D., Baxter, A.E., Vella, L.A., et al. (2020). Comprehensive mapping of immune perturbations associated with severe COVID-19. Sci Immunol. *5*, eabd7114.

Le Bert, N., Tan, A.T., Kunasegaran, K., Tham, C.Y.L., Hafezi, M., Chia, A., Chng, M.H.Y., Lin, M., Tan, N., Linster, M., et al. (2020). SARS-CoV-2-specific T cell immunity in cases of COVID-19 and SARS, and uninfected controls. Nature *584*, 457–462.

Liao, M., Liu, Y., Yuan, J., Wen, Y., Xu, G., Zhao, J., Cheng, L., Li, J., Wang, X., Wang, F., et al. (2020). Single-cell landscape of bronchoalveolar immune cells in patients with COVID-19. Nat. Med. *26*, 842–844.

Mathew, D., Giles, J.R., Baxter, A.E., Oldridge, D.A., Greenplate, A.R., Wu, J.E., Alanio, C., Kuri-Cervantes, L., Pampena, M.B., D'Andrea, K., et al. (2020). Deep immune profiling of COVID-19 patients reveals distinct immunotypes with therapeutic implications. Science. *369*, eabc8511.

Mazzoni, A., Salvati, L., Maggi, L., Capone, M., Vanni, A., Spinicci, M., Mencarini, J., Caporale, R., Peruzzi, B., Antonelli, A., et al. (2020). Impaired immune cell cytotoxicity in severe COVID-19 is IL-6 dependent. J. Clin. Invest. *130*, 4694–4703.

McLane, L.M., Abdel-Hakeem, M.S., and Wherry, E.J. (2019). CD8 T Cell Exhaustion During Chronic Viral Infection and Cancer. Annu. Rev. Immunol. *37*, 457–495.

National Institutes of Health (2020). COVID-19 Treatment Guidelines Panel. Coronavirus Disease 2019 (COVID-19) Treatment Guidelines. https://www.covid19treatmentguidelines.nih.gov/.

Park, S.H., Shin, E.C., Capone, S., Caggiari, L., De Re, V., Nicosia, A., Folgori, A., and Rehermann, B. (2012). Successful vaccination induces multifunctional memory T-cell precursors associated with early control of hepatitis C virus. Gastroenterology *143*, 1048, 60.e4.

Sekine, T., Perez-Potti, A., Rivera-Ballesteros, O., Strålin, K., Gorin, J.B., Olsson, A., Llewellyn-Lacey, S., Kamal, H., Bogdanovic, G., Muschiol, S., et al.; Karolinska COVID-19 Study Group (2020). Robust T cell immunity in convalescent individuals with asymptomatic or mild COVID-19. Cell *183*, 158–168.e14.

Shin, E.C., Park, S.H., Nascimbeni, M., Major, M., Caggiari, L., de Re, V., Feinstone, S.M., Rice, C.M., and Rehermann, B. (2013). The frequency of CD127(+) hepatitis C virus (HCV)-specific T cells but not the expression of exhaustion markers predicts the outcome of acute HCV infection. J. Virol. *87*, 4772–4777.

Singer, M., Wang, C., Cong, L., Marjanovic, N.D., Kowalczyk, M.S., Zhang, H., Nyman, J., Sakuishi, K., Kurtulus, S., Gennert, D., et al. (2016). A Distinct Gene Module for Dysfunction Uncoupled from Activation in Tumor-Infiltrating T Cells. Cell *166*, 1500–1511.e9.

Song, J.W., Zhang, C., Fan, X., Meng, F.P., Xu, Z., Xia, P., Cao, W.J., Yang, T., Dai, X.P., Wang, S.Y., et al. (2020). Immunological and inflammatory profiles in mild and severe cases of COVID-19. Nat. Commun. *11*, 3410.

Weiskopf, D., Schmitz, K.S., Raadsen, M.P., Grifoni, A., Okba, N.M.A., Endeman, H., van den Akker, J.P.C., Molenkamp, R., Koopmans, M.P.G., van Gorp, E.C.M., et al. (2020). Phenotype and kinetics of SARS-CoV-2-specific T cells in COVID-19 patients with acute respiratory distress syndrome. Sci Immunol. *5*, eabd2071.

Wherry, E.J., and Kurachi, M. (2015). Molecular and cellular insights into T cell exhaustion. Nat. Rev. Immunol. *15*, 486–499.

World Health Organization (2020). Coronavirus disease 2019 (COVID-19) Situation Report-209. (16 August 2020). https://www.who.int/docs/default-source/coronaviruse/situation-reports/20200816-covid-19-sitrep-209.pdf?sfvrsn=5dde1ca2_2.

Zheng, H.Y., Zhang, M., Yang, C.X., Zhang, N., Wang, X.C., Yang, X.P., Dong, X.Q., and Zheng, Y.T. (2020a). Elevated exhaustion levels and reduced functional diversity of T cells in peripheral blood may predict severe progression in COVID-19 patients. Cell. Mol. Immunol. *17*, 541–543.

Zheng, M., Gao, Y., Wang, G., Song, G., Liu, S., Sun, D., Xu, Y., and Tian, Z. (2020b). Functional exhaustion of antiviral lymphocytes in COVID-19 patients. Cell. Mol. Immunol. *17*, 533–535.

STAR★METHODS

KEY RESOURCES TABLE

REAGENT or RESOURCE	SOURCE	IDENTIFIER
Antibodies		
BV510 anti-human CD3 (clone UCHT1)	BD Biosciences	Cat# 563109; RRID: AB_2732053
BV605 anti-human CD8 (clone SK1)	BD Biosciences	Cat# 564116; RRID: AB_2744466
BV421 anti-human CD127 (clone HIL-7R-M21)	BD Biosciences	Cat# 562436; RRID: AB_11151911
V450 anti-human Granzyme B (clone GB11)	BD Biosciences	Cat# 561151; RRID: AB_10565977
AF700 anti-human CD38 (clone HIT2)	BD Biosciences	Cat# 560676; RRID: AB_1727472
BB515 anti-human CD38 (clone HIT2)	BD Biosciences	Cat# 564498; RRID: AB_2744374
PE-CF594 anti-Human CD19 (clone HIB19)	BD Biosciences	Cat# 562294; RRID: AB_11154408
BB515 anti-human CD45RA (clone HI100)	BD Biosciences	Cat# 564552; RRID: AB_2738841
PerCP-Cy5.5 anti-human CCR7 (clone 150503)	BD Biosciences	Cat# 561144; RRID: AB_10562553
FITC anti-human HLA A2 (clone BB7.2)	BD Biosciences	Cat# 551285; RRID: AB_394130
PerCP-Cy5.5 anti-human HLA-DR (clone L243)	BioLegend	Cat# 307630; RRID: AB_893567
APC-Cy7 anti-human HLA-DR (clone L243)	BioLegend	Cat# 307618; RRID: AB_493586
BV785 anti-human CD28 (clone CD28.2)	BioLegend	Cat# 302950; RRID: AB_2632607
PE anti-human PD-1 (clone EH12.2H7)	BioLegend	Cat# 329906; RRID: AB_940483
APC-Cy7 anti-human CD127 (clone A019D5)	BioLegend	Cat# 351348; RRID: AB_2629572
AF700 anti-human Ki-67 (clone Ki-67)	BioLegend	Cat# 350530; RRID: AB_2564040
BV785 anti-human TIM-3 (clone F38-2E2)	BioLegend	Cat# 345032; RRID: AB_2565833
PE-eFluor 610 anti-human CD14 (clone 61D3)	Thermo Fisher Scientific	Cat# 61-0149-42; RRID: AB_2574534
PE-Cy7 anti-human KLRG1 (clone 13F12F2)	Thermo Fisher Scientific	Cat# 25-9488-42; RRID: AB_2573546
PE-Cy7 anti-human Perforin (clone dG9)	Thermo Fisher Scientific	Cat# 25-9994-42; RRID: AB_2573574
Biological Samples		
Blood samples from individuals with SARS-CoV-2 infection	Chungbuk National University hospital, Samsung Medical Center, Severance hospital, Wonju Severance Christian Hospital, Seoul National University Bundang Hospital, Seoul Medical Center, Ansan Hospital	N/A
Chemicals, Peptides, and Recombinant Proteins		
Lymphocyte separation medium	Corning	Cat# 25-072-CV
Fetal bovine serum	Corning	Cat# 35-015-CV
Dimethyl sulfoxide	Sigma-Aldrich	Cat# D8418
7-AAD	BD Biosciences	Cat# 559925
SARS-CoV-2 $S_{269-277}$ YLQPRTFLL peptide	Mimotopes	Customized
CMV $pp65_{495-503}$ NLVPMVATV peptide	Peptron	Customized
Influenza A MP_{58-66} GILGFVFTL peptide	Peptron	Customized
Critical Commercial Assays		
LIVE/DEAD red fluorescent reactive dye	Invitrogen	Cat# L34972
Celltrace Violet	Invitrogen	Cat# C34557
IFN-γ Secretion Assay-Detection Kits, human	Miltenyi Biotec	Cat# 130-090-433
CD8 MicroBeads, human	Miltenyi Biotec	Cat# 130-045-201
FoxP3 staining buffer kit	Invitrogen	Cat# 00-5523-00
Software and Algorithms		
FlowJo software version 10.7	FlowJo LLC	https://www.flowjo.com/

(*Continued on next page*)

Continued		
REAGENT or RESOURCE	SOURCE	IDENTIFIER
Prism version 8	Graphpad	https://www.graphpad.com/
MUSCLE	Edgar 2004	N/A
Other		
APC YLQPRTFLL (SARS-CoV-2 S_{269}) HLA-A*0201 Pentamer	Proimmune	Cat# 4339
APC FIAGLIAIV (SARS-CoV-2 S_{1220}) HLA-A*0201 Pentamer	Proimmune	Cat# 4321
APC RLQSLQTYV (SARS-CoV-2 S_{1000}) HLA-A*0201 Pentamer	Proimmune	Cat# 4358
APC LITGRLQSL (SARS-CoV-2 S_{996}) HLA-A*0201 Pentamer	Proimmune	Cat# 4323
APC ALNTLVKQL (SARS-CoV-2 S_{958}) HLA-A*0201 Pentamer	Proimmune	Cat# 4322
APC RLNEVAKNL (SARS-CoV-2 S_{1185}) HLA-A*0201 Dextramer	Immudex	Customized
APC TLACFVLAAV (SARS-CoV-2 M_{61}) HLA-A*0201 Dextramer	Immudex	Customized
APC LLLDRLNQL (SARS-CoV-2 N_{22}) HLA-A*0201 Dextramer	Immudex	Customized
APC NLVPMVATV (CMV $pp65_{495}$) HLA-A*0201 Dextramer	Immudex	Cat# WB2132
APC GILGFVFTL (IAV MP_{58}) HLA-A*0201 Dextramer	Immudex	Cat# WB2161

RESOURCE AVAILABILITY

Lead Contact

Further information and requests for resources and reagents should be directed to and will be fulfilled by the Lead Contact, Eui-Cheol Shin (ecshin@kaist.ac.kr).

Materials Availability

This study did not generate new unique reagents.

Data and Code Availability

The published article includes all data generated during this study. All codes are freely available at source.

EXPERIMENTAL MODEL AND SUBJECT DETAILS

Patients and Specimens

In this study, 235 patients diagnosed with SARS-CoV-2 infection were enrolled from Chungbuk National University Hospital, Samsung Medical Center, Severance Hospital, Wonju Severance Christian Hospital, Seoul National University Bundang Hospital, Seoul Medical Center, and Ansan Hospital. Peripheral blood (PB) was obtained from all patients with SARS-CoV-2 infection. SARS-CoV-2 RNA was detected in specimens from the patients' nasopharyngeal swabs by multiplex real-time RT-PCR using the Allplex 2019-nCoV Assay kit (Seegene, Seoul, Republic of Korea) or PowerCheck 2019-nCoV RT PCR kit (KogeneBiotech, Seoul, Republic of Korea). In this assay, the E, N, and RdRP genes of SARS-CoV-2 were amplified and Ct values obtained for each gene. In the present study, we categorized patients into two groups: non-severe and severe. Non-severe patients comprised asymptomatic, mild, and moderate illness, whereas severe patients comprised severe and critical illness as defined by the NIH severity of illness categories (National Institutes of Health, 2020). The convalescent phase was defined as the period after the negative conversion of SARS-CoV-2 RNA in real-time RT-PCR. The early and late convalescent phases were defined as the period within and after the first 14 days following the negative conversion of SARS-CoV-2 RNA, respectively. PB was also obtained from 7 healthy donors without exposure to SARS-CoV-2. This study was reviewed and approved by the institutional review board of all participating institutions and conducted according to the principles of the Declaration of Helsinki. Informed consent was obtained from all donors and patients.

PBMCs were isolated by density gradient centrifugation using Lymphocyte Separation Medium (Corning, NY, USA). After isolation, the cells were cryopreserved in fetal bovine serum (Corning) with 10% dimethyl sulfoxide (Sigma-Aldrich, St. Louis, USA) until use.

METHOD DETAILS

MHC class I multimer staining and multi-color flow cytometry

PBMCs were stained with APC-conjugated MHC class I multimers for 15 min at room temperature, washed, and then stained with fluorochrome-conjugated antibodies for specific surface markers for 10 min at room temperature. Dead cells were excluded using LIVE/DEAD red fluorescent reactive dye (Invitrogen, Carlsbad, CA, USA). In some experiments, cells were fixed and permeabilized using the FoxP3 staining buffer kit (Invitrogen), and then stained for intracellular markers for 30 min at 4°C. Multi-color flow cytometry was performed using an LSR II instrument (BD Biosciences, San Jose, CA, USA) and the data analyzed in FlowJo software (FlowJo

LLC, Ashland, OR, USA). The fluorochrome-conjugated MHC class I multimers and monoclonal antibodies used in this study are listed in the KEY RESOURCES TABLE.

Sequence alignment

Complete protein sequences for the spike protein of SARS-CoV-2 and other coronaviruses known to infect humans were downloaded from the NCBI database (NCBI database: YP_009724390.1, YP_009825051.1, YP_009047204.1, YP_009555241.1, YP_173238.1, NP_073551.1, YP_003767.1). MUSCLE algorithm (Edgar, 2004) was used to align multiple sequences.

Cell sorting

$CD8^+$ T cells were enriched from PBMCs using magnetic-activated cell sorting CD8 microbeads (Miltenyi Biotec, Auburn, CA, USA) according to the manufacturer's instructions. Enriched $CD8^+$ T cells were stained with PE-conjugated anti-PD-1 antibody (Bio-Legend, San Diego, CA, USA) and 7-AAD (BD Biosciences), and then live $PD\text{-}1^+CD8^+$ and $PD\text{-}1^-CD8^+$ T cells were sorted using an ARIA II instrument (BD Biosciences).

Cytokine secretion assay

PBMCs, sorted $PD\text{-}1^+CD8^+$ T cells, or sorted $PD\text{-}1^-CD8^+$ T cells were stained with APC-conjugated multimers for 15 min at room temperature, washed, and stimulated with 1 μg/mL epitope peptide for 5.5 h. In experiments with sorted $PD\text{-}1^+CD8^+$ T cells or $PD\text{-}1^-CD8^+$ T cells, autologous $CD8^-$ cells were used as feeder cells. After subsequent incubation with IFN-γ catch reagents (Miltenyi Biotec) for 55 min at 37°C on a rotator, the cells were stained with FITC-labeled anti-IFN-γ detection reagents (Miltenyi Biotec) for 10 min on ice. Additional staining was performed with APC-conjugated multimers and antibodies for specific surface markers.

Proliferation assay

PBMCs were stained with a cell division tracking dye, CTV (Invitrogen), according to the manufacturer's instructions. CTV-labeled cells were then stimulated with 10 μg/mL peptide for 7 days. On day 7, the cells were stained with MHC class I multimers and proliferation assessed by flow cytometry.

Statistical analysis

Statistical analyses were performed using GraphPad Prism version 8 for Windows (GraphPad Software, San Diego, CA, USA). Significance was set at $p < 0.05$. The Wilcoxon signed-rank test was used to compare data between two paired groups and the Mann–Whitney U test to compare data between two unpaired groups. To assess the significance of correlation, the Spearman correlation test was used.